Journal of Diabetes Science and Technology
Volume 7, Issue 2, March 2013

ORIGINAL ARTICLE

Enhancing the Sensitivity of Needle-Implantable Electrochemical Glucose Sensors via Surface Rebuilding

Santhisagar Vaddiraju, Ph.D.,[1,2] Allen Legassey, B.S.,[1] Liangliang Qiang, M.S.,[2] Yan Wang, B.S.,[3] Diane J. Burgess, Ph.D.,[3] and Fotios Papadimitrakopoulos, Ph.D.[2,4]

Abstract

Objective:

Needle-implantable sensors have shown to provide reliable continuous glucose monitoring for diabetes management. In order to reduce tissue injury during sensor implantation, there is a constant need for device size reduction, which imposes challenges in terms of sensitivity and reliability, as part of decreasing signal-to-noise and increasing layer complexity. Herein, we report sensitivity enhancement *via* electrochemical surface rebuilding of the working electrode (WE), which creates a three-dimensional nanoporous configuration with increased surface area.

Methods:

The gold WE was electrochemically rebuilt to render its surface nanoporous followed by decoration with platinum nanoparticles. The efficacy of such process was studied using sensor sensitivity against hydrogen peroxide (H_2O_2). For glucose detection, the WE was further coated with five layers, namely, (1) polyphenol, (2) glucose oxidase, (3) polyurethane, (4) catalase, and (5) dexamethasone-releasing poly(vinyl alcohol)/poly(lactic-co-glycolic acid) composite. The amperometric response of the glucose sensor was noted *in vitro* and *in vivo*.

Results:

Scanning electron microscopy revealed that electrochemical rebuilding of the WE produced a nanoporous morphology that resulted in a 20-fold enhancement in H_2O_2 sensitivity, while retaining >98% selectivity. This afforded a 4–5-fold increase in overall glucose response of the glucose sensor when compared with a control sensor with no surface rebuilding and fittable only within an 18 G needle. The sensor was able to reproducibly track *in vivo* glycemic events, despite the large background currents typically encountered during animal testing.

Conclusion:

Enhanced sensor performance in terms of sensitivity and large signal-to-noise ratio has been attained *via* electrochemical rebuilding of the WE. This approach also bypasses the need for conventional and nanostructured mediators currently employed to enhance sensor performance.

J Diabetes Sci Technol 2013;7(2):441–451

Author Affiliations: [1]Biorasis Inc. Technology Incubation Program, University of Connecticut, Storrs, Connecticut; [2]Polymer Program, Institute of Materials Science, University of Connecticut, Storrs, Connecticut; [3]Department of Pharmaceutical Sciences, University of Connecticut, Storrs, Connecticut; and [4]Department of Chemistry, University of Connecticut, Storrs, Connecticut

Abbreviations: (AgCl) silver chloride, (CV) cyclic voltammetry, (FBR) foreign body response, (GO_x) glucose oxidase, (H_2O_2) hydrogen peroxide, ($K_3Fe[CN]_6$) potassium ferricyanide, (KCl) potassium chloride, (NP) nanoparticle, (PLGA) poly(lactic-co-glycolic acid), (PPh) polyphenol, (PVA) poly(vinyl alcohol), (SC) subcutaneous, (WE) working electrode

Keywords: electrochemical, implantable glucose sensor, membranes, needle-implantable, sensitivity, surface etching

Corresponding Author: Fotios Papadimitrakopoulos, Ph.D., Polymer Program, Institute of Material Science, U-3136, University of Connecticut, Storrs, CT 06269; email address papadim@mail.ims.uconn.edu

Introduction

Continuous glucose monitoring in conjunction with a closed-loop insulin delivery could help in diabetes management and significantly reduce the risk of associated complications such as renal failure and blindness.[1] For this purpose, various glucose monitoring devices are being developed that can be classified as noninvasive, minimally invasive, and invasive.[2] Invasive devices based on subcutaneously implanted amperometric glucose sensors have received widespread scientific and commercial attention because of their simple operating principle and propensity to miniaturization.[2]

First-generation Clark-based amperometric sensors employ a glucose oxidase (GO_x) enzyme immobilized on top of the working electrode (WE).[3,4] The flavin adenine dinucleotide redox cofactor of GO_x catalyzes the oxidation of glucose to glucarolactone, as shown in **Equations (1)** and **(2)**:

$$Glucose + \mathrm{GO_x}(FAD) \rightarrow Glucorolactone + GO_x(FADH_2) \tag{1}$$

$$\mathrm{GO_x}(FADH_2) + O_2 \rightarrow GO_x(FAD) + H_2O_2 \tag{2}$$

The generated hydrogen peroxide (H_2O_2) is amperometrically assessed on the surface of the WE in accordance with **Equation (3)**:

$$\mathrm{H_2}O_2 \xrightarrow{+V} 2H^+ + O_2 + 2e^- \tag{3}$$

The reliability of such subcutaneously implanted amperometric glucose sensors hinges on addressing the following interdependent factors:[2,4–6]

(i) Saturation of sensor response at high glucose concentrations due to the inadequate amount of oxygen present (only 0.18 mM as compared with 5.6 mM of physiological glucose concentration [glucose/O_2 ratio ≅ 30][7]), rendering **Equation (2)** oxygen limited.[4,6]

(ii) Suboptimal *in vivo* performance due to post-inflammation effects such as biofouling and foreign body response (FBR), leading to the formation of a fibrotic capsule that attenuates the diffusion of glucose and O_2 toward the WE.[8–11] The extent of FBR is proportional to the magnitude of injury that occurred during device implantation, dependent on the size of the implantable sensor.[8,12]

The first issue is typically addressed *via* the use of glucose flux limiting[13–21] and/or O_2-supplementing[21] membranes, while the latter concern is typically alleviated by employing biocompatible[12,22–30] and/or inflammation-suppressing coatings.[31–38] These approaches succeed at the expense of decreased sensitivity.[2,4,20,29,39]

In order to minimize the injury inflicted during sensor implantation (that reduces the extent of FBR), device miniaturization also becomes important.[39,40] Miniaturization, however, stands as another impediment for sensitivity, because reduction in the area of the WE generally leads to weaker signal intensity that approaches noise levels. To mitigate this challenge, biosensors have resorted to the use of high surface area nanostructured materials [e.g., mediators, nanotubes, metal nanoparticles (NPs)] along with appropriately engineered substrates.[39,41–43] Toxicity concerns associated with the use of such nanostructured materials could ultimately hinder their application in implantable sensor configurations.[39] In addition, the need for high resilience against mechanical movement of the sensor in the dynamic *in vivo* environment restricts the design space to needle-implantable devices with high flexibility.[17,20,28,29,44,45]

In this article, we report on the fabrication and characterization of a needle-type glucose sensor that comfortably fits within a 26 G needle (with an inner diameter of 260 μm). Despite the reduction in the size of the WE, a robust *in vivo* and *in vitro* performance is demonstrated with sensor sensitivity and selectivity equivalent to or better than the currently reported needle-type sensors with larger surface areas.[17,20,28,29,44,45] This has been achieved through electrochemical rebuilding of the gold WE, that together with platinum NPs and conformal layer engineering provided a 20-fold increase in electrocatalytic activity against H_2O_2 detection. *In vitro* evaluation has shown that a glucose sensor utilizing such surface rebuilding showed a 4–5-fold increase in sensor response along with high selectivity (greater than 98%), high linearity (greater than 30 mM), and low response times (40 ± 6 s). In addition, short-term *in vivo* study in a rat model has shown that the glucose sensor reproducibly tracks the glycemic events, despite the large background noise in its microenvironment. Such high *in vitro* and *in vivo* performance together with adequate mechanical integrity and flexibility needed for long-term operation renders this "rebuilt" sensor promising for continuous glucose monitoring.

Experimental

Materials

Glucose oxidase enzyme, catalase, glutaraldehyde, phenol, bovine serum albumin, D-glucose, and Selectophore polyurethane (Tecoflex^{TM}) were purchased from Sigma. Poly(vinyl alcohol) (PVA; 99% hydrolyzed, molecular weight 133 kDa) was obtained from Polysciences Inc. Poly(lactic-co-glycolic acid) (PLGA) Resomer RG503H 50:50 was a gift from Boehringr-Ingelheim.

Experimental Methods

To prepare PVA solutions, 5% weight/volume aqueous solution of PVA was preheated to approximately 80 °C to facilitate complete polymer dissolution.

Dexamethasone-loaded microspheres were prepared by an oil-in-water emulsion solvent extraction/evaporation technique as described previously.[33]

Needle-type sensors were fabricated by coiling a 50 μm gold wire on top of a 125 μm platinum wire, which served as the WE. The starting surface area of the gold WE is approximately 0.18 mm^2. The reference electrode was made by coiling a 50 μm silver wire in close proximity to the WE and converting its surface to silver chloride (AgCl) *via* galvanometry.

Surface rebuilding of the gold WE was achieved by immersing it in a 2 M sodium hydroxide solution and by applying a square wave potential waveform from -1.0 to +0.8 V versus Ag/AgCl.[46]

Deposition of platinum NPs was achieved by immersing the rebuilt gold WE in 10 mM chloropatinic acid/0.1 M hydrogen chloride solution and by applying a bias of -0.05 V for 60 s.[47]

For the fabrication of glucose sensors, the WE was sequentially coated with five different layers [namely, polyphenol (PPh), GO_x, polyurethane, catalase, and PVA/PLGA composite] as reported before.[21,33]

Cyclic voltammetry (CV) was performed in a quiescent, oxygen-free solution of 10 mM potassium ferricyanide [$K_3Fe(CN)_6$] in 0.1 potassium chloride (KCl) at a scan rate of 10 mV/s.

In vitro amperometric experiments were performed as reported earlier.[21,33] In brief, the response of the sensor to either H_2O_2 (or glucose) was obtained by applying a potential of 0.5 V to the WE and by raising the concentration from 0 to 0.5 mM and 2 to 35 mM for H_2O_2 and glucose, respectively.

In vivo amperometric experiments were performed in young anesthetized male Sprague rats (150–175 g) as per Institutional Animal Care and Use Committee guidelines. The sensor is implanted into the subcutaneous (SC) tissue and is connected to a CHI workstation through two thin insulated wires that exit through the skin. The sensors were polarized for 2 h to obtain a stable signal,[28] following which 0.2 ml of sterile 50% dextrose was administered intraperitoneally. The response corresponding to the glycemic event of the rat was recorded continuously, while the tail-vein blood glucose readings were obtained periodically. Following the first glycemic event, a second glucose injection (0.4 ml of 50% dextrose) was administered, and the procedure was repeated again before proceeding to a third injection of 0.6 ml of 50% dextrose.

Results and Discussion

Sensitivity enhancement is a critical necessity for the higher noise levels typically encountered with *in vivo* biosensors. With this in mind, electrochemical surface rebuilding of gold was utilized to enhance surface area of the WE.[46] This converts the smooth surface of the WE to nanoporous morphology *via* the repeated etching and redeposition of the gold surface when subjected to a square waveform (at +0.8 and –1.0 V, at a frequency of 50 Hz for exposure times of 450 to 7200 s) in a 2 M sodium hydroxide solution.[46] During the application of the positive +0.8 V cycle, the gold surface gets oxidized, and the gold ions form a soluble complex with OH^-, to be redeposited at the negative -1.0 V bias interval. The resulting nanoporous gold morphology is attained *via* templation by the oxygen and hydrogen microbubbles that are generated during the positive and negative potential cycles, respectively.[46]

Cyclic voltammetry was used to assess the efficacy of the surface rebuilding process toward enhancing surface area of the gold WE. Typically, CV in a redox mediator [such as $K_3Fe(CN)_6$] gives rise to anodic and cathodic peaks corresponding to the oxidation and reduction of the mediator. The intensity of the redox peak current is proportional to surface area, assuming that the electrocatalytic activity of the surface remains the same. **Figure 1** shows the CV of the sensors before and after the surface rebuilding step, obtained in 10mM $K_3Fe(CN)_6$ and 0.1M KCl at a scan rate of 50 mV/s. The well-defined anodic and cathodic waves, produced by the oxidation and reduction of $K_3Fe(CN)_6$, are retained following surface rebuilding of the gold WE. However, the intensity of the waves are substantially increased (by 9–10-fold), providing an initial indication of the enhancement in the surface area of the WE.

Effect of Etching Time

Having confirmed the utility of surface rebuilding toward increasing surface area, the effect of etching time has been investigated. For this sensor, sensitivity toward H_2O_2 has been used as an assessment parameter since the electro-oxidation of H_2O_2 is the key step for the amperometric glucose sensing [**Equations (1)–(3)**]. **Figure 2** shows the changes in sensor sensitivity toward H_2O_2 as a function of electrochemical surface rebuilding time of the gold WE.

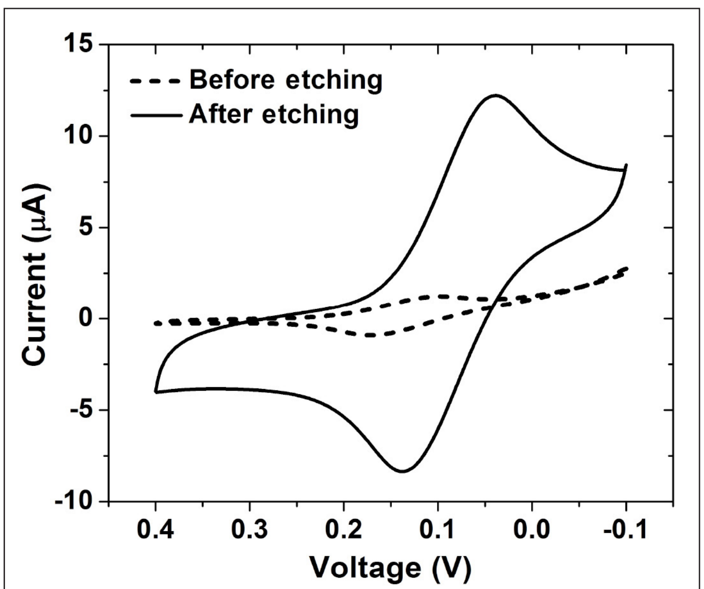

Figure 1. Cyclic voltammograms of the gold WE (starting area of 0.569 mm^2) in 10 mM $K_3(FeCN_6)$/0.1 M KCl aqueous solution at 10 mV/s scanning rate before (dotted curve) and after (solid curve) the electrochemical rebuilding process.

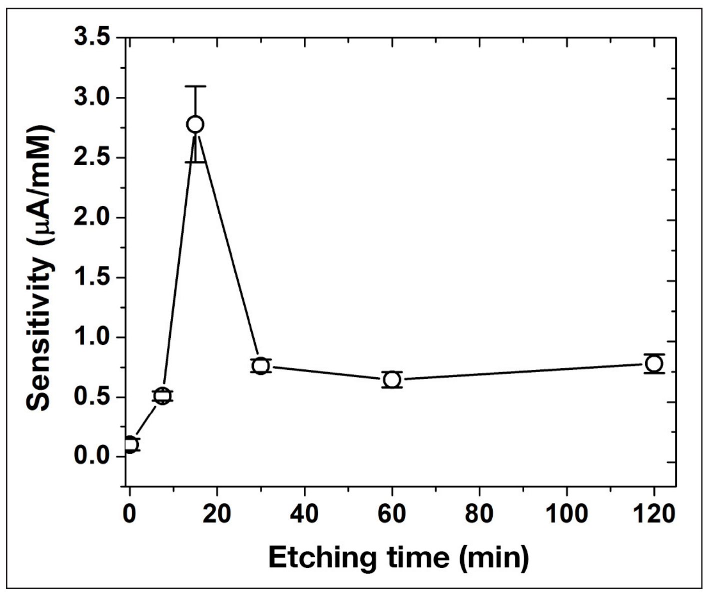

Figure 2. Hydrogen peroxide sensitivity of the electrochemical surface rebuilt gold WE (with initial surface area of 0.569 mm2) as a function of etching time using a square waveform (at +0.8 and –1.0 V at a frequency of 50 Hz for exposure times of 450 to 7200 s) in a 2 M sodium hydroxide solution.

The H_2O_2 sensitivity increased with increasing etching times and peaked at 15 min before dropping to a lower value and saturating at longer time periods. The peak sensitivity value is 20-fold higher when compared with the starting one. Such increase in sensor sensitivity is twice more than that recorded by the CV measurement in **Figure 1**. This can be attributed to the smaller size of H_2O_2 as compared with $K_3Fe(CN)_6$, which greatly improves the three-dimensional diffusion and analyte transfer to the nanoporous gold electrodes.[48]

To further understand the origin in peak sensitivity observed at 15 min of electrochemical gold rebuilding, the nanoporous morphologies of the WE were assessed via scanning electron microscopy. **Figure 3** depicts the surface morphology of the gold WE as a function of etching time. Here the following differences can be noted:

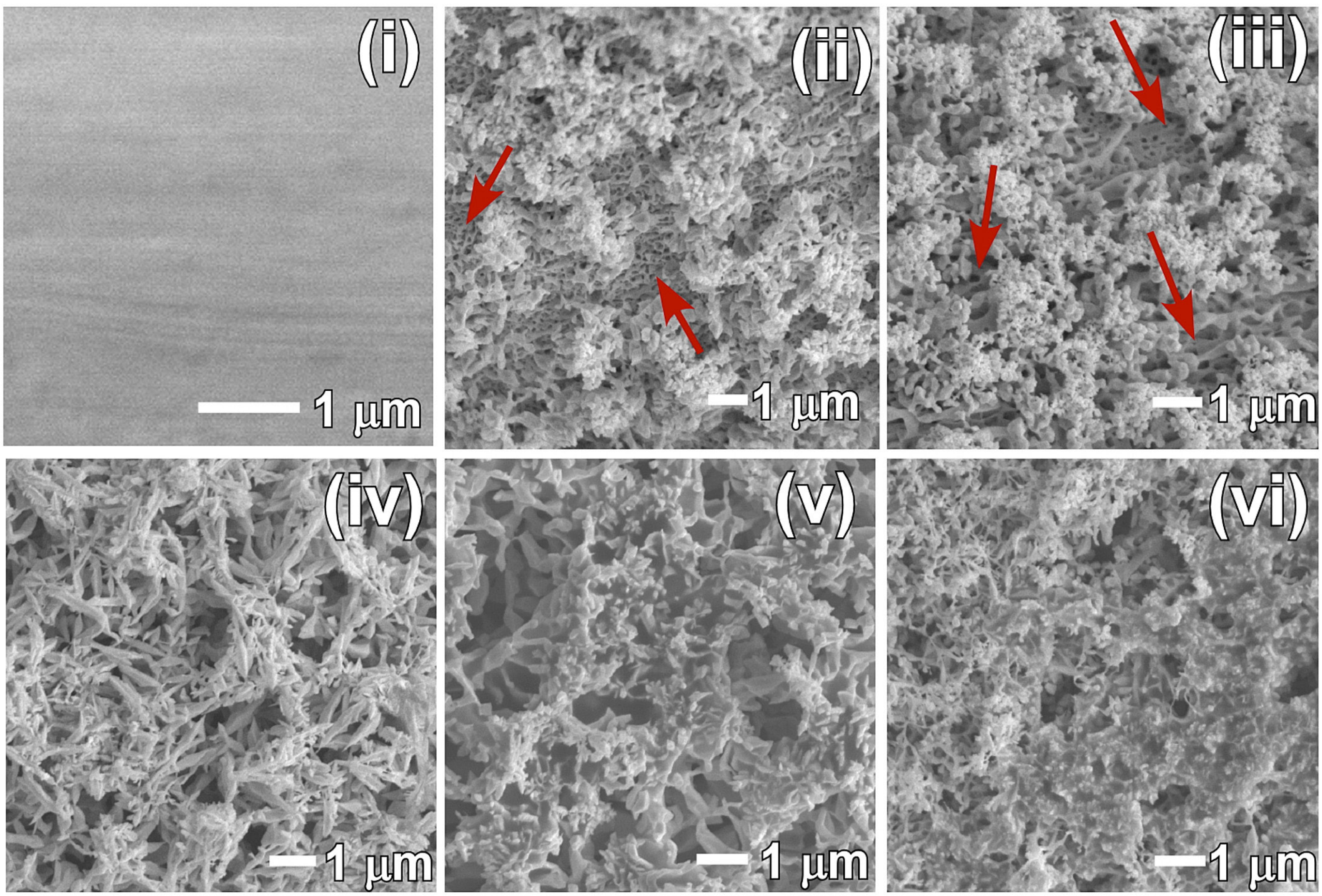

Figure 3. Scanning electron microscopic images of gold WEs (i) before and after electrochemical rebuilding for (ii) 7.5, (iii) 15, (iv) 30, (v) 60, and (vi) 120 min.

(i) Among all electrochemical rebuilding times investigated, the 7.5 and 15 min etching times produced a "flowery" structure with an underlying nanoporous substructure (depicted with red arrows), both of which contribute to enhancement in surface area. Moreover, the underlying substructure for the 15 min etching time is more pronounced and porous compared with the 7.5 min etching time.

(ii) At etching times beyond 15 min, the outer "flowery" structure started to fuse together, disrupting the nanoscale morphology, and finally, at 120 min, most of the nanoscale features fused with each other, contributing to decrease in surface area.

These findings provide a visual understanding of the origin of peak sensitivity obtained at 15 min electrochemical rebuilding. Based on this, all further experiments were conducted using 15 min electrochemical rebuilding.

Further Improvement in Device Sensitivity Using Electrodeposited Platinum Nanoparticles

Even though the surface rebuilding *via* etching enhances the gold surface area, its utility toward sensor fabrication is hindered due to the inherent electrochemical instability of gold surfaces.[47,48] For this, the rebuilt gold surface was further decorated with platinum NPs in accordance with Reference 48.

The sensitivity increase afforded by the platinum NPs was investigated against electro-oxidation of H_2O_2. **Figure 4** illustrates the H_2O_2 sensitivity obtained for the same starting gold WE (0.569 mm^2) as a function of gold rebuilding and electrodeposition of platinum NPs. For the purpose of comparison, the sensitivities of two more configurations were investigated, namely, (i) bare gold and (ii) bare platinum, both of which were electrodeposited with platinum NPs. As illustrated in **Figure 4**, surface rebuilding of gold electrodes followed by decoration with platinum NPs leads to sensitivity enhancement by nearly two orders of magnitude higher than bare gold electrodes. This implies that deposition of platinum NPs does not completely clog the pores created through surface rebuilding, in accordance with previous findings.[48] More importantly, the sensitivity of the platinum NP-decorated gold rebuilt electrode is twice as high as that of bare platinum decorated with platinum NPs, thus providing substantial cost reduction in starting materials.

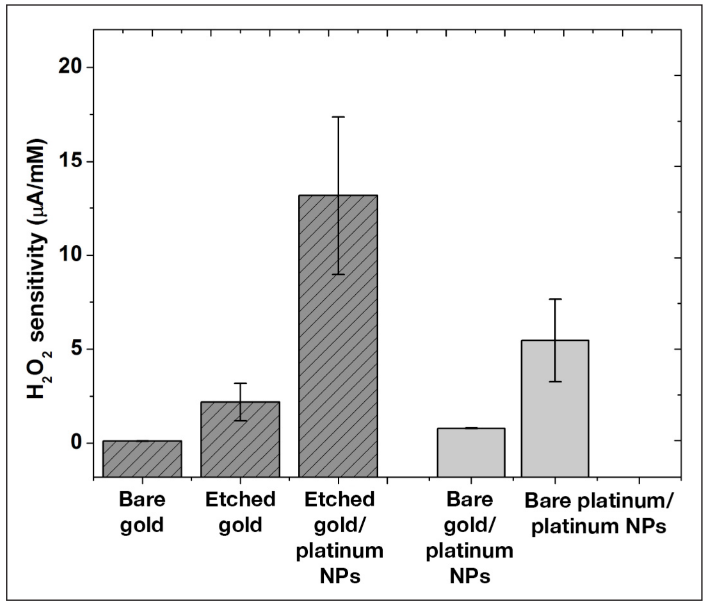

Figure 4. Hydrogen peroxide sensitivity (at +0.5 V versus Ag/AgCl reference) for various WEs (see text for details). Au, gold; Pt, platinum.

Glucose Sensor Architecture

Having demonstrated a simplistic methodology to improve sensor sensitivity toward H_2O_2, the same has been used to realize a high-performance glucose sensor. For this, the rebuilt gold WE was decorated with platinum NPs and with various functional layers for reliable glucose detection. **Figures 5A** and **5B** show a photograph and schematic cross section of the sensor. **Figure 5C** illustrates the various layers of the WE, whose function are described here:

(i) A conformal electropolymerized PPh layer (~10 nm) intended to prevent the diffusion of large molecular weight interferences (e.g., acetaminophen, ascorbic acid, uric acid) to the WE, where they are likely to get oxidized;[39]

(ii) Glucose oxidase enzyme layer (20–25 μm) that was immobilized *via* glutaraldehyde cross linking;

(iii) A 1–2 μm polyurethane film intended to offset the large glucose-to-O_2 ratio within the SC tissue and improve sensor linearity;[39,45,49]

(iv) A thin layer of catalase (5–10 μm) to convert H_2O_2 to O_2 and enable facile extraction of H_2O_2 from the GO_x enzyme layer[19,20,45,49,50] (this provides a faster response time, minimal hysteresis,[20] excess O_2 to decrease the glucose-to-oxygen ratio, as well as preventing H_2O_2 outer-diffusion to reduce irritation to the surrounding SC tissue); and[51]

(v) A thicker (approximately 50 μm) composite coating of PVA hydrogel and dexamethasone-containing PLGA microspheres, cross linked in place through the application of three repetitive freezing and thawing cycles[33]

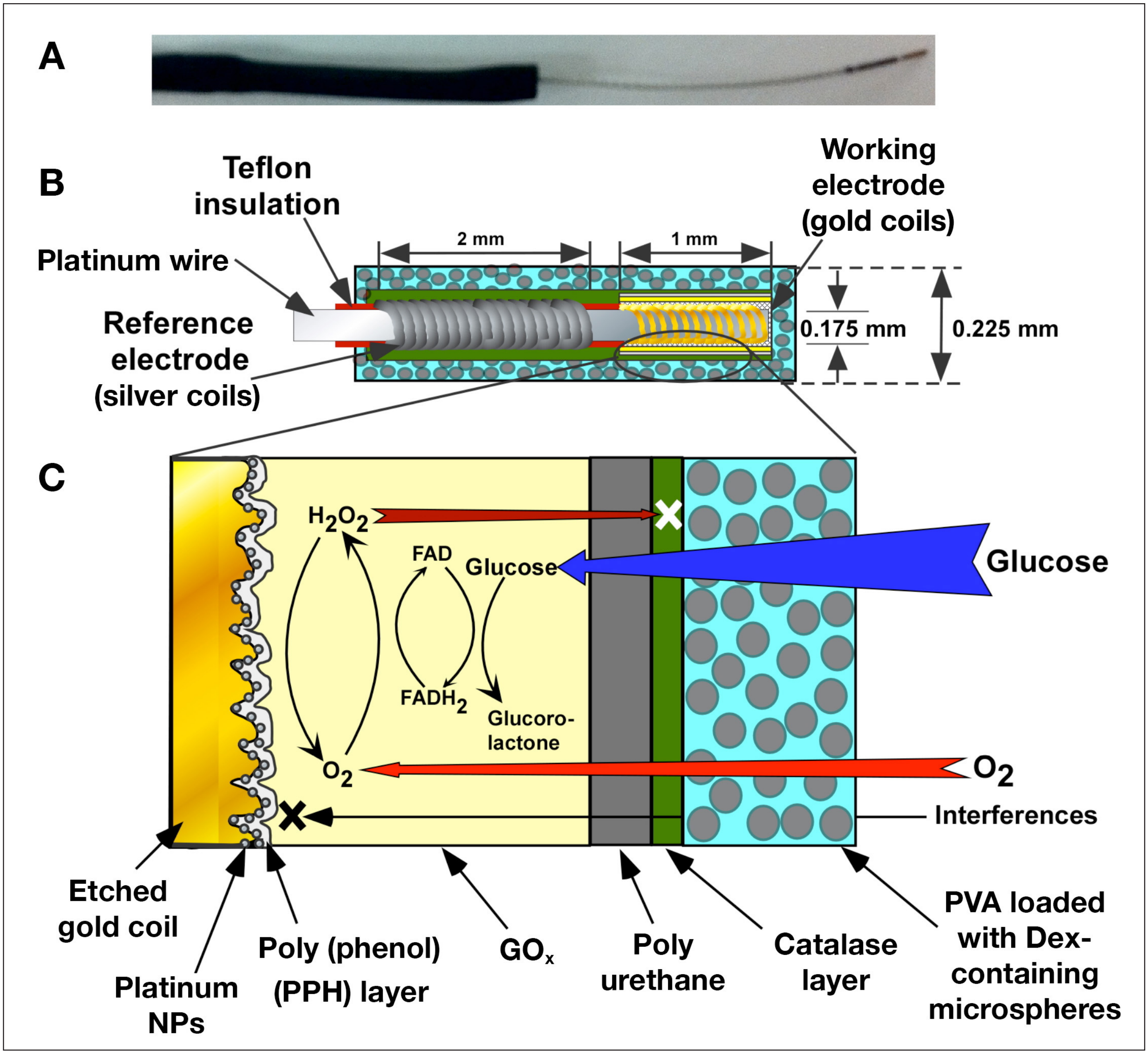

Figure 5. (A) Photograph and **(B)** schematic cross section of the needle-implantable glucose sensor under investigation. **(C)** The various functional layers that compose the WE are shown (not to scale). FAD, flavin adenine dinucleotide.

(the PVA hydrogel provides a continuous pathway for diffusion of glucose toward the WE while the microspheres afford a controlled release of dexamethasone through PLGA degradation).[33,45,49]

Glucose Sensor Characteristics

Sensor Response Time, Linearity, and Sensitivity

Figure 6A illustrates the *in vitro* amperometric response of the fabricated glucose sensor to sequential additions of glucose. As evident, the sensor responded quickly and reproducibly to each of the glucose additions with a response time of 40 ± 8 s (time to achieve 90% of saturation current), similar to our earlier reports.[20] **Figure 6B** illustrates the saturation amperometric response versus glucose concentration, as obtained from the data of **Figure 6A**. Also shown in **Figure 6B** is the amperometric response versus glucose concentration curve for a control sensor that did undergo WE surface rebuilding but possessed platinum NPs as well as the five functional layers described earlier (**Figure 5C**). In both cases, the addition of glucose resulted in a linear increase of response for glucose concentrations as high as 30 mM, which is well beyond the physiological range. However, for any glucose concentration, the response of the "surface rebuilt" sensor is 4–5-fold higher than the control sensor, signifying the increase in surface area achieved through surface rebuilding. The *in vitro* glucose sensitivity of this "surface rebuilt" 26 G-fittable sensor as obtained from **Figure 6B** is 70 nA/mM/mm^2. **Table 1** compares the sensitivities obtained from the present work with those reported for similar "needle-type" glucose sensors. The sensitivity obtained from the present 26 G-fittable sensor is superior to previously reported ones (at least seven times better than sensors with the similar area). More importantly, it should be noted that such superior sensitivity has been obtained despite the presence of five functional layers as compared with three or four in previous reports.[20,28,29] This enhanced sensor sensitivity is primarily due to the surface rebuilding of the WE that substantially increases its surface area (see **Figure 3**).

<u>*Sensor Selectivity*</u>

While the incorporation of PPh on top of WE has shown to be effective in block interferences at smoother WEs,[20] the same may not hold true for nanoporous WEs if this film is not conformal. This calls for a reinvestigation of the efficacy of PPh at nanoporous WE toward rejection of interferences. For this, we have chosen acetaminophen as a model interference substance, as it has been shown to be the most difficult one to be screened.[4] **Figure 6C** shows the response of sequential additions of 5 mM glucose and 0.1 mM acetaminophen when operated at 0.5 V. While the sensor shows a distinct and reproducible increase for glucose additions, negligible to no response is witnessed for acetaminophen additions (i.e., less than 2% of its amperometric response on bare platinum electrode; data not shown). This indicates that the electropolymerized PPh film affords uniform coating over gold rebuilt WE, which is decorated with platinum NPs. Moreover, such electropolymerized PPh film possesses similar porosity to that deposited on planar platinum surfaces, with pores sufficiently large to allow H_2O_2 to pass through, yet small enough to prevent the diffusion of the larger sized acetaminophen. This also alludes to the fact that such PPh film also eliminates any direct oxidation of glucose on the highly electrocatalytic etched gold/platinum NP-based WE.[53]

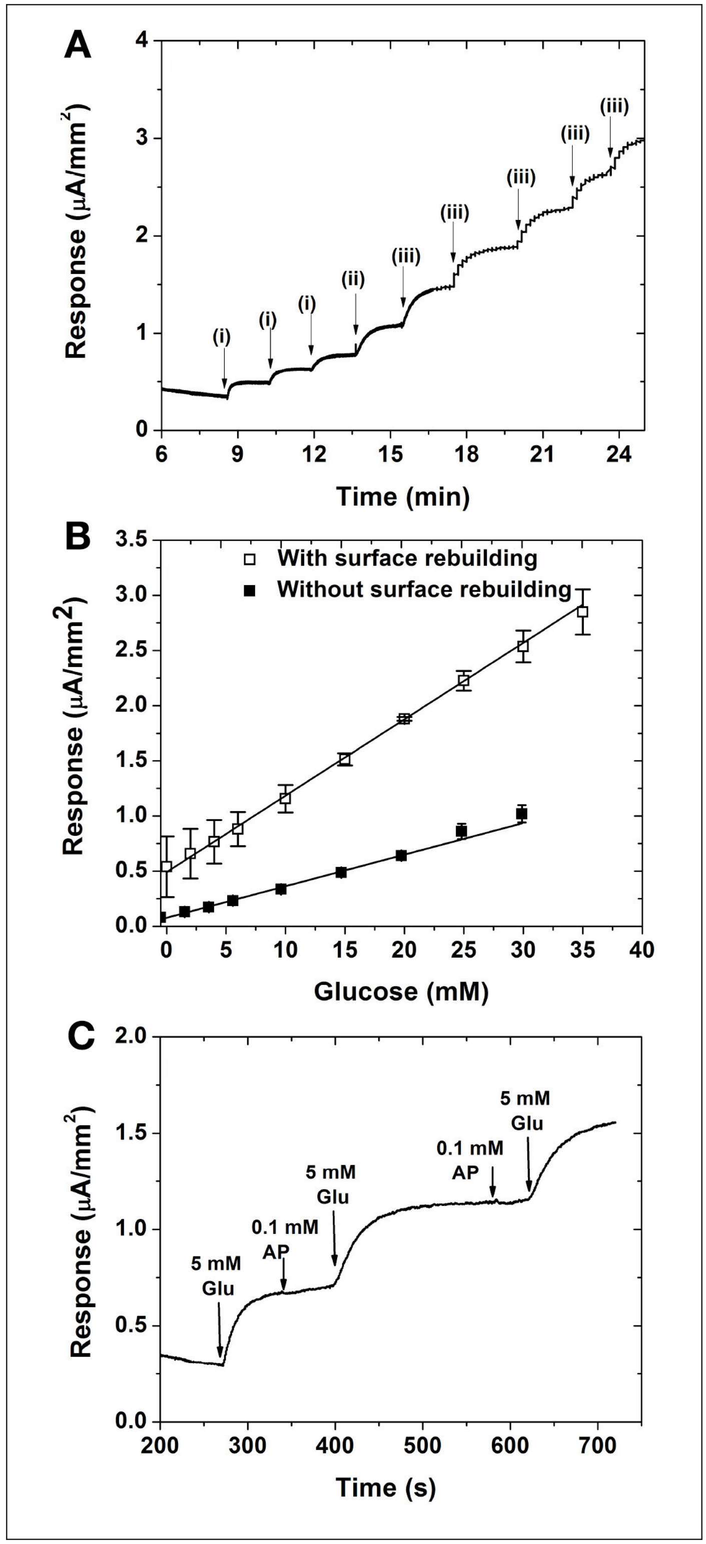

Figure 6. *In vitro* characteristics of the needle-implantable glucose sensor under study. **(A)** Transient sensor response to sequential additions of (i) 2, (ii) 4, and (iii) 5 mM glucose. **(B)** Saturation amperometric response as a function of glucose concentrations of the surface rebuilt sensor (open squares) and the control sensor with no surface rebuilding (closed squares). **(C)** Transient sensor response to sequential additions of 5 mM of glucose and 0.1 mM of acetaminophen (interference agent). AP, acetaminophen; Glu, glucose.

In Vivo *Glucose Sensor Performance Test*

Reproducible operation *in vivo* presents the ultimate test for the functionality of any implantable glucose sensor. With this in mind, the *in vivo* performance of the glucose sensor was evaluated for a short period of time (3–4 h) in an unconscious (anesthetized) rat. **Figure 7** shows the amperometric response from the SC implanted sensor for duration of approximately 4 h, along with the plasma glucose values determined from tail vein sampling. In response to an intraperitoneal injection of dextrose, the plasma glucose levels started to increase and peaked at around 10 min before coming back to normal levels. The sensor response closely tracked the plasma glucose levels. Similarly, in response to the subsequent second and third glucose injections, both the plasma glucose and sensor response showed a steady increase followed by a decrease. An average lag of approximately 5 ± 2 min (mean from the three glycemic peaks shown in **Figure 7**) was observed between the plasma glucose and the change in the sensor current. This lag phase is due to (i) the physical time lag between the interstitial fluid and plasma, which can vary between 4 and 10 min and (ii) the time needed for the sensor to reach saturation value following a change in the glucose concentration (i.e., the sensor response time). Considering the fact that *in vitro* sensor response time (**Figure 6A**) is only 40 s, it can be easily concluded that the lag phase observed in **Figure 7** is due to physical lag time between the plasma and interstitial fluid glycemic events.[54] Overall, the short-term results of **Figure 7** confirms the efficacy of the 26 G-fittable sensor to detect *in vivo* glycemic events and confirms its efficacy in tracking glycemic events *in vivo* despite a small WE and the presence of large background noises in its microenvironment. Currently, we are focused on evaluating the long-term (1 month) performance of this sensor in both *in vitro* and *in vivo* environments.

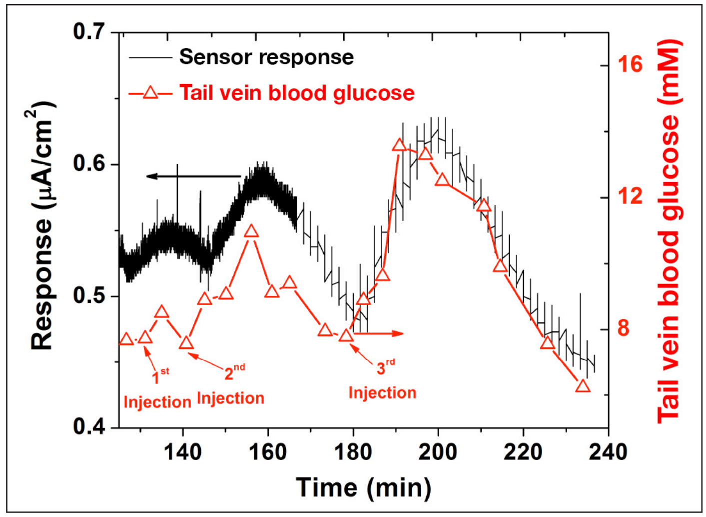

Figure 7. Real-time *in vivo* response (left ordinate, black) of the glucose sensor to three glycemic events induced by intraperitoneal dextrose injections overlaid against the tail vein plasma glucose levels (right ordinate, red).

Conclusions

Electrochemical rebuilding of a gold WE produces a nano-porous morphology with enhanced surface area and results in a 20-fold increase in sensitivity toward H_2O_2 detection. The inclusion of platinum NPs on top of the "rebuilt" WE further improves its H_2O_2 sensitivity by another six-fold. The electropolymerization of phenol on top of such nanostructured electrode produces a thin, conformal, and pinhole-free layer of PPh that blocks redox interferences from interferences. Subsequent layering with GO_x (for glucose sensing), polyurethane (for limiting glucose flux), catalase (for removing excess H_2O_2), and PVA hydrogel/PLGA microspheres composite (for inflammation suppression) produces a highly reliable sensor with sensitivity as high as 70 nA/mM/cm^2 (4–5-fold increase in response when compared with a control sensor with nosurface rebuilding) and linearity up to 35 mM of glucose. Such a sensor is small enough to fit in a 26 G catheter and exhibits a six-fold higher sensitivity than previously reported needle-implantable devices. Short-term *in vivo* study has shown that the sensor can reproducibly track glycemic events despite the large background currents typically encountered during animal testing. Such performance proves that surface rebuilding of the WE can produce adequate sensitivity to afford device miniaturization as well as to bypass the need for mediators. Moreover, this approach is also amenable to a robust fabrication of miniaturized implantable glucose sensors.

References:

1. The Diabetes Control and Complications Trial Research Group. The effect of intensive treatment of diabetes on the development and progression of long-term complications in insulin-dependent diabetes mellitus. N Engl J Med. 1993;329(14):977–86.
2. Vaddiraju S, Burgess DJ, Tomazos I, Jain FC, Papadimitrakopoulos F. Technologies for continuous glucose monitoring: current problems and future promises. J Diabetes Sci Technol. 2010;4(6):1540–62.
3. Clark LC Jr, Lyons C. Electrode systems for continuous monitoring in cardiovascular surgery. Ann N Y Acad Sci. 1962;102:29–45.
4. Wilson GS, Gifford R. Biosensors for real-time *in vivo* measurements. Biosens Bioelectron. 2005;20(12):2388–403.
5. Wang J. Glucose biosensors: 40 years of advances and challenges. Electroanalysis. 2001;13(12):983–8.
6. Wang J. *In vivo* glucose monitoring: towards 'Sense and Act' feedback-loop individualized medical systems. Talanta. 2008;75(3):636–41.
7. Vaddiraju S, Burgess DJ, Tomazos I, Jain FC, Papadimitrakopoulos F. Technologies for continuous glucose monitoring: current problems and future promises. J Diabetes Sci Technol. 2010;4(6):1540–62.
8. Anderson JM. Biological responses to materials. Annu Rev Mater Res. 2001;31(1):81–110.
9. Anderson JM, Rodriguez A, Chang DT. Foreign body reaction to biomaterials. Semin Immunol. 2008;20(2):86–100.
10. Wisniewski N, Klitzman B, Miller B, Reichert WM. Decreased analyte transport through implanted membranes: differentiation of biofouling from tissue effects. J Biomed Mater Res. 2001;57(4):513–21.
11. Wisniewski N, Reichert M. Methods for reducing biosensor membrane biofouling. Colloids Surf B Biointerfaces. 2000;18(3-4):197–219.
12. Kvist PH, Iburg T, Aalbaek B, Gerstenberg M, Schoier C, Kaastrup P, Buch-Rasmussen T, Hasselager E, Jensen HE. Biocompatibility of an enzyme-based, electrochemical glucose sensor for short-term implantation in the subcutis. Diabetes Technol Ther. 2006;8(5):546–59.
13. Bindra DS, Zhang Y, Wilson GS, Sternberg R, Thévenot DR, Moatti D, Reach G. Design and *in vitro* studies of a needle-type glucose sensor for subcutaneous monitoring. Anal Chem. 1991;63(17):1692–6.
14. Galeska I, Chattopadhyay D, Moussy F, Papadimitrakopoulos F. Calcification-resistant Nafion/Fe3+ assemblies for implantable biosensors. Biomacromolecules. 2000;1(2):202–7.
15. Harrison DJ, Turner RF, Baltes HP. Characterization of perfluorosulfonic acid polymer coated enzyme electrodes and a miniaturized integrated potentiostat for glucose analysis in whole blood. Anal Chem. 1988;60(19):2002–7.
16. Maines A, Ashworth D, Vadgama P. Diffusion restricting outer membranes for greatly extended linearity measurements with glucose oxidase enzyme electrodes. Anal Chim Acta. 1996;333(3):223–31.
17. Moussy F, Harrison DJ, O'Brien DW, Rajotte RV. Performance of subcutaneously implanted needle-type glucose sensors employing a novel trilayer coating. Anal Chem. 1993;65(15):2072–7.
18. Praveen SS, Hanumantha R, Belovich JM, Davis BL. Novel hyaluronic acid coating for potential use in glucose sensor design. Diabetes Technol Ther. 2003;5(3):393–9.
19. Tipnis R, Vaddiraju S, Jain F, Burgess DJ, Papadimitrakopoulos F. Layer-by-layer assembled semipermeable membrane for amperometric glucose sensors. J Diabetes Sci Technol. 2007;1(2):193–200.
20. Vaddiraju S, Legassey A, Wang Y, Qiang L, Burgess DJ, Jain F, Papadimitrakopoulos F. Design and fabrication of a high-performance electrochemical glucose sensor. J Diabetes Sci Technol. 2011;5(5):1044–51.
21. Vaddiraju S, Singh H, Burgess DJ, Jain FC, Papadimitrakopoulos F. Enhanced glucose sensor linearity using poly(vinyl alcohol) hydrogels. J Diabetes Sci Technol. 2009;3(4):863–74.
22. Galeska I, Hickey T, Moussy F, Kreutzer D, Papadimitrakopoulos F. Characterization and biocompatibility studies of novel humic acids based films as membrane material for an implantable glucose sensor. Biomacromolecules. 2001;2(4):1249–55.
23. Gant RM, Hou Y, Grunlan MA, Coté GL. Development of a self-cleaning sensor membrane for implantable biosensors. J Biomed Mater Res A. 2009;90(3):695–701.
24. Ishihara K, Tanaka S, Furukawa N, Kurita K, Nakabayashi N. Improved blood compatibility of segmented polyurethanes by polymeric additives having phospholipid polar groups. I. Molecular design of polymeric additives and their functions. J Biomed Mater Res. 1996;32(3):391–9.
25. Kyrolainen M, Rigsby P, Eddy S, Vadgama P. Bio-/haemocompatibility: implications and outcomes for sensors? Acta Anaesthesiol Scand Suppl. 1995;104:55–60.
26. Yang W, Xue H, Carr LR, Wang J, Jiang S. Zwitterionic poly(carboxybetaine) hydrogels for glucose biosensors in complex media. Biosens Bioelectron. 2011;26(5):2454–9.
27. Yang Y, Zhang SF, Kingston MA, Jones G, Wright G, Spencer SA. Glucose sensor with improved haemocompatibilty. Biosens Bioelectron. 2000;15(5-6):221–6.
28. Yu B, Long N, Moussy Y, Moussy F. A long-term flexible minimally-invasive implantable glucose biosensor based on an epoxy-enhanced polyurethane membrane. Biosens Bioelectron. 2006;21(12):2275–82.
29. Yu B, Wang C, Ju YM, West L, Harmon J, Moussy Y, Moussy F. Use of hydrogel coating to improve the performance of implanted glucose sensors. Biosens Bioelectron. 2008;23(8):1278–84.
30. Gough DA, Kumosa LS, Routh TL, Lin JT, Lucisano JY. Function of an implanted tissue glucose sensor for more than 1 year in animals. Sci Transl Med. 2010;2(42):42ra53.

31. Bhardwaj U, Sura R, Papadimitrakopoulos F, Burgess DJ. PLGA/PVA hydrogel composites for long-term inflammation control following s.c. implantation. Int J Pharm. 2010;384(1-2):78–86.

32. Bhardwaj U, Sura R, Papadimitrakopoulos F, Burgess DJ. Controlling acute inflammation with fast releasing dexamethasone-PLGA microsphere/pva hydrogel composites for implantable devices. J Diabetes Sci Technol. 2007;1(1):8–17.

33. Galeska I, Kim TK, Patil SD, Bhardwaj U, Chatttopadhyay D, Papadimitrakopoulos F, Burgess DJ. Controlled release of dexamethasone from PLGA microspheres embedded within polyacid-containing PVA hydrogels. AAPS J. 2005;7(1):E231–40.

34. Gifford R, Batchelor MM, Lee Y, Gokulrangan G, Meyerhoff ME, Wilson GS. Mediation of *in vivo* glucose sensor inflammatory response via nitric oxide release. J Biomed Mater Res A. 2005;75(4):755–66.

35. Hetrick EM, Prichard HL, Klitzman B, Schoenfisch MH. Reduced foreign body response at nitric oxide-releasing subcutaneous implants. Biomaterials. 2007;28(31):4571–80.

36. Koh A, Nichols SP, Schoenfisch MH. Glucose sensor membranes for mitigating the foreign body response. J Diabetes Sci Technol. 2011;5(5):1052–9.

37. Norton LW, Koschwanez HE, Wisniewski NA, Klitzman B, Reichert WM. Vascular endothelial growth factor and dexamethasone release from nonfouling sensor coatings affect the foreign body response. J Biomed Mater Res A. 2007;81(4):858–69.

38. Patil SD, Papadmitrakopoulos F, Burgess DJ. Concurrent delivery of dexamethasone and VEGF for localized inflammation control and angiogenesis. J Control Release. 2007;117(1):68–79.

39. Vaddiraju S, Tomazos I, Burgess DJ, Jain FC, Papadimitrakopoulos F. Emerging synergy between nanotechnology and implantable biosensors: a review. Biosens Bioelectron. 2010;25(7):1553–65.

40. Li C, Han J, Ahn CH. Flexible biosensors on spirally rolled micro tube for cardiovascular *in vivo* monitoring. Biosens Bioelectron. 2007;22(9-10):1988–93.

41. Adiga S, Curtiss L, Elam J, Pellin M, Shih CC, Shih CM, Lin SJ, Su YY, Gittard S, Zhang J, Narayan R. Nanoporous materials for biomedical devices. JOM J Minerals Metals Materials Soc. 2008;60(3):26–32.

42. Ainslie KM, Desai TA. Microfabricated implants for applications in therapeutic delivery, tissue engineering, and biosensing. Lab Chip. 2008;8(11):1864–78.

43. Ainslie KM, Sharma G, Dyer MA, Grimes CA, Pishko MV. Attenuation of protein adsorption on static and oscillating magnetostrictive nanowires. Nano Lett. 2005;5(9):1852–6.

44. Chen X, Matsumoto N, Hu Y, Wilson GS. Electrochemically mediated electrodeposition/electropolymerization to yield a glucose microbiosensor with improved characteristics. Anal Chem. 2002;74(2):368–72.

45. Croce RA Jr, Vaddiraju S, Kondo J, Wang Y, Zuo L, Zhu K, Islam SK, Burgess DJ, Papadimitrakopoulos F, Jain FC. A miniaturized transcutaneous system for continuous glucose monitoring. Biomed Microdevices. 2012. Epub ahead of print.

46. Huang W, Wang M, Zheng J, Li Z. Facile fabrication of multifunctional three-dimensional hierarchical porous gold films via surface rebuilding. J Phys Chem. 2009;113(5):1800–5.

47. Qiang L, Vaddiraju S, Rusling JF, Papadimitrakopoulos F. Highly sensitive and reusable Pt-black microfluidic electrodes for long-term electrochemical sensing. Biosens Bioelectron. 2010;26(2):682–8.

48. Qiang L, Vaddiraju S, Patel D, Papadimitrakopoulos F. Edge-plane microwire electrodes for highly sensitive H 2O 2 and glucose detection. Biosens Bioelectron. 2011;26(9):3755–60.

49. Vaddiraju S, Wang Y, Qiang L, Burgess DJ, Papadimitrakopoulos F. Microsphere erosion in outer hydrogel membranes creating macroscopic porosity to counter biofouling-induced sensor degradation. Anal Chem. 2012;84(20):8837–45.

50. Vaddiraju S, Burgess DJ, Jain FC, Papadimitrakopoulos F. The role of H2O2 outer diffusion on the performance of implantable glucose sensors. Biosens Bioelectron. 2009;24(6):1557–62.

51. Watt BE, Proudfoot AT, Vale JA. Hydrogen peroxide poisoning. Toxicol Rev. 2004;23(1):51–7.

52. Ward WK, Jansen LB, Anderson E, Reach G, Klein JC, Wilson GS. A new amperometric glucose microsensor: *in vitro* and short-term *in vivo* evaluation. Biosens Bioelectron. 2002;17(3):181–9.

53. Marinčić L, Soeldner JS, Colton CK, Giner J, Morris S. Electrochemical glucose oxidation on a platinized platinum electrode in Krebs-ringer solution. I. Potentiodynamic studies. J Electrochem Soc. 1979;126(1):43–9.

54. Kovatchev BP, Gonder-Frederick LA, Cox DJ, Clarke WL. Evaluating the accuracy of continuous glucose-monitoring sensors: continuous glucose-error grid analysis illustrated by TheraSense Freestyle Navigator data. Diabetes Care. 2004;27(8):1922–8.